

Understanding fluid turbulence through numerical simulations

D.O. Gómez^{1,2} & P.D. Mininni¹



<http://astro.df.uba.ar>



Abdus Salam ICTP, october 27, 2003



Theoretical description

✓ Paradigm: incompressible Navier-Stokes equation

$$\begin{aligned} \partial_t \bar{u} &= -(\bar{u} \cdot \nabla) \bar{u} - \frac{1}{\rho} \nabla p + \nu \nabla^2 \bar{u} \\ \nabla \cdot \bar{u} &= 0 \end{aligned}$$

✓ It is a nonlinear and dissipative PDE. We get rid of the pressure by integrating the curl of this equation, and using

$$\omega = \nabla \times \bar{u} \quad \bar{u} = (\nabla \times)^{-1} \omega$$

for appropriate boundary conditions.

✓ Energy is an ideal invariant ($E = \text{const.}$ for $\nu = 0$)

$$E = \frac{1}{2} \rho \int d^3 r |\bar{u}|^2$$



The Reynolds number

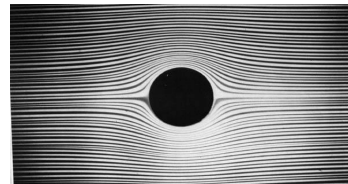
$$R = \frac{U \cdot L}{\nu}$$

- ✓ Turbulence \Rightarrow efficient mixing
- ✓ Diffusion equation $\Rightarrow \partial_t u = \nu \nabla^2 u$
- ✓ Molecular diffusion $\Rightarrow v_{mol} \approx u_{th} \cdot \ell_{mfp}$
- ✓ Turbulent diffusion $\Rightarrow v_{turb} \approx u \cdot L$
- ✓ Efficiency $\Rightarrow \frac{v_{turb}}{v_{mol}} = \frac{U \cdot L}{\nu} = R$



Symmetries

✓ $R = \frac{U \cdot L}{\nu} \ll 1$

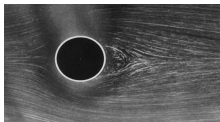


$$x \leftrightarrow -x$$

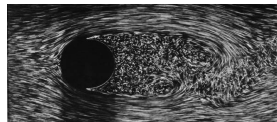
- ✓ symmetries $\begin{cases} t \leftrightarrow t + \tau \\ y \leftrightarrow -y \end{cases}$



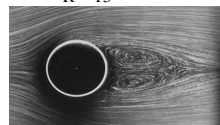
Symmetry breaking



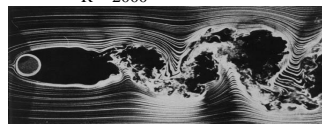
R = 13



R = 2000



R = 26

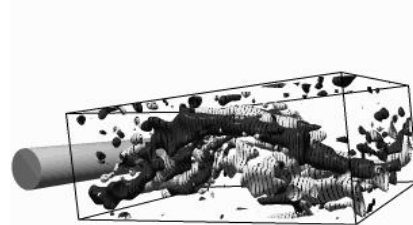


R = 10000



Symmetry breaking

✓ In 3D, the vorticity past a cylinder looks like



Fluid instabilities

- ✓ ... for instance, Kelvin-Helmholtz
- ✓ Linear stability: $A(t) = A_0 e^{\Gamma(\vec{k}, R)t}$
- ✓ Generation of new scales
- ✓ Nonlinear mode coupling

Instabilities: Boundary layers

- ✓ Laminar structures in the neighbourhood of walls
 - ↳ dominated by viscosity
- ✓ Stationary equilibrium (Blasius)
 - ↳ $\delta(x) = 1.73 \sqrt{\frac{\nu x}{u_0}}$
- ✓ Non-ideal instability: it disappears for $R = \infty$

Rotating cilinder (in water) at R=100

Instabilities: Jets

Instabilities: Taylor-Couette

Flow between two cylinders.

The external cylinder remains static while the internal one rotates at:

(a) $\omega = 1.16 \omega_{crit} \Rightarrow k_z$

(b) $\omega = 8.5 \omega_{crit} \Rightarrow k_\theta = 6$

Instabilities: Rayleigh-Benard

zoom

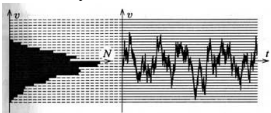
- ✓ Thermal instability:
 - ↳ $\vec{g} \cdot \nabla T > 0$

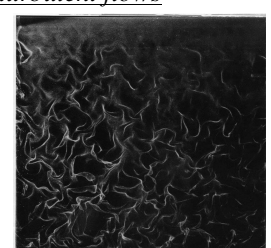
Instabilities: 2D simulations

- ✓ You are looking at vorticity vs. position and time.

Kelvin-Helmholtz Jet instability

Randomness of turbulent flows

- ✓ Velocity vs. time
 
- ✓ Definition of statistical averages

$$\langle \dots \rangle = \lim_{N \rightarrow \infty} \frac{1}{N} \sum_1^N (\dots)$$
 for N repetitions of an experiment.
 
- ✓ Assuming ergodicity

$$\left\{ \begin{array}{l} \langle \dots \rangle = \frac{1}{L} \int d'x (\dots) \quad \text{for homogeneous turbulence} \\ \langle \dots \rangle = \frac{1}{T} \int_0^T (\dots) \quad \text{for stationary turbulence} \end{array} \right.$$

Empirical laws: the 2/3 law

- ✓ The relative velocity between two points separated by l is

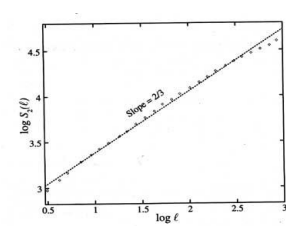
$$S_2(\ell) \equiv \langle |\delta v(\ell)|^2 \rangle \approx \ell^{2/3}$$

- ✓ A large number of experiments and simulations confirm this law.

Fig. 5.1. log-log plot of the second order structure function in the time domain for data from the S1 wind tunnel of ONERA. Courtesy Y. Gagne and E. Hopfinger.

Empirical laws: the 2/3 law

- ✓ ... both for the longitudinal structure function

$$S_2^{\parallel}(\ell) \equiv \langle |\delta v_{\parallel}(\ell)|^2 \rangle \approx \ell^{2/3}, \quad \delta v_{\parallel}(\ell) = (\bar{v}(F+\ell) - \bar{v}(F)) \cdot \frac{\ell}{\ell}$$
- ✓ ... and the transverse structure function.

$$S_2^{\perp}(\ell) \equiv \langle |\delta \bar{v}_{\perp}(\ell)|^2 \rangle \approx \ell^{2/3}, \quad \delta \bar{v}_{\perp}(\ell) = \delta \bar{v} - \delta v_{\parallel} \frac{\bar{\ell}}{\ell}$$
- ✓ We define the structure function of order n as

$$S_n(\ell) \equiv \langle |\delta \bar{v}(\ell)|^n \rangle \approx (\ell \epsilon)^{n/3}$$
- ✓ This is a very important experimental result, which is consistent with Kolmogorov's spectrum (Gagne et al. 1991).

Empirical laws: Richardson's law

- ✓ To study the diffusion rate of tracers in the atmosphere, we can follow the separation between two Lagrangian points in time

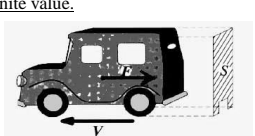
$$\ell^2(t) \equiv \langle |\bar{r}_2(t) - \bar{r}_1(t)|^2 \rangle$$
- ✓ Richardson (1926), found that this separation grows like

$$\sigma \equiv \frac{1}{2} \frac{d\ell^2}{dt} \approx \ell^{5/3}$$
- ✓ This empirical law is also consistent with Kolmogorov

$$\sigma = \ell \frac{d\ell}{dt} = \ell \delta v(\ell) \approx \ell (\ell \epsilon)^{1/3}$$

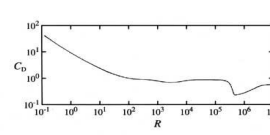
Empirical laws: finite dissipation rate

- ✓ In the limit of negligible viscosity, the energy dissipation rate converges to a non-negligible and finite value.
- ✓ Experimentally, the drag force over an object of transverse section S and velocity V , is

$$F = \frac{c_D}{2} \rho S V^2, \quad c_D : \text{const.}$$

- ✓ The momentum transferred from the fluid in dt is

$$dp = F dt = \rho V S (V dt)$$
 and $\frac{c_D}{2}$ measures the efficiency of this transfer.

Empirical laws: finite dissipation rate

- ✓ Experimentally, c_D shows the following behavior:
 
- ✓ At high Reynolds, except for $R=10^6$ (separation of the boundary layer) is $c_D = \text{const.}$ The dissipated energy per unit mass is

$$\epsilon = - \frac{\bar{F} \cdot \bar{V}}{\rho S \ell^3} = \frac{c_D}{2} \frac{V^3}{S \ell^2} \quad \text{independent of } R.$$

Fig. 5.11. Variation of drag coefficient with Reynolds number for circular cylinders.

Energy cascade

- ✓ The energy cascade can be visualized as the successive break up of vortices into smaller vortices.

Fig. 7.2. The cascade according to the Kolmogorov 1941 theory. Notice that at each step the eddies are space-filling.

Energy cascade

- ✓ The energy balance for scales larger than $\ell = \kappa^{-1}$

$$\partial E_x + \Pi_x = -2\nu\Omega_x + F_x$$
 where $F_x = \int_0^x dk k^2 \bar{f}_i \bullet \bar{u}_i$

$$E_x = \int_0^x dk k^2 E_i$$

$$\Omega_x = \int_0^x dk k^4 E_i$$

- ✓ In the inertial range

$$\Pi_x = F_x \equiv \epsilon$$
- ✓ At the injection region and in a stationary regime

$$\Pi_x = F_x$$
- ✓ In the dissipation range

$$\Pi_x = -2\nu\Omega_x + \epsilon$$

Kolmogorov's hypotheses

- ✓ **Hypothesis 1:** In the limit $R \rightarrow \infty$ all the NS symmetries, which were broken by the mechanisms that generated turbulence, are reestablished at a statistical level and only for the microscale.
- ✓ **Hypothesis 2:** For $R \rightarrow \infty$, the flow displays a finite energy dissipation rate ($0 < \epsilon < \infty$)
- ✓ **Hypothesis 3:** For $R \rightarrow \infty$, all statistical properties of the microscale, are universally determined by the scale ℓ and by the energy dissipation rate ϵ .

Kolmogorov spectrum

- ✓ Energy cascade energy flux toward high k vortex breakdown
- ✓ Scale invariance energy flux in k: $\epsilon_k \approx \frac{u_k^2}{\tau_k}$ energy power spectrum: $E_k \approx \frac{u_k^2}{k}$

$$\tau_k \approx \frac{1}{ku_k}, \quad \epsilon_k \approx \frac{u_k^2}{\tau_k} = cte$$

$$u_k \approx \left(\frac{\epsilon}{k}\right)^{1/3}, \quad E_k \approx \frac{u_k^2}{k} = \epsilon^{2/3} k^{-5/3}$$

Kolmogorov spectrum

- ✓ One of the symmetries of ideal NS is scale invariance (**Hyp. 1**)

$$\bar{v} \rightarrow \lambda \bar{v} \quad \bar{u} \rightarrow \lambda^h \bar{u} \quad t \rightarrow \lambda^{-h} t \quad p \rightarrow \lambda^{2h} p$$
- ✓ According to **Hyp. 2**, in the inertial range

$$\Pi_x \approx \kappa u_x^3 = \epsilon \quad \Rightarrow \quad h = \frac{1}{3}$$
- ✓ From **Hyp. 3**, the energy power spectrum becomes

$$E(k) \approx \epsilon^\alpha \ell^\beta$$

$$\frac{(L/T)^2}{1/L} \approx \left(\frac{L}{T}\right)^\alpha L^\beta \quad \Rightarrow \quad \alpha = \frac{2}{3}, \quad \beta = \frac{5}{3} \quad \Rightarrow \quad E(k) \approx \epsilon^{2/3} k^{-5/3}$$

The dissipative range

- ✓ In the range of sizes for which

$$v_{turb} \approx v_{mol} \Leftrightarrow R_\nu = \frac{\ell u_\ell}{\nu} \approx 1$$
- ✓ $u_\ell \approx (\epsilon \ell)^\alpha \Rightarrow \ell_{dis} \approx \left(\frac{\nu^3}{\epsilon}\right)^{1/2}$
- ✓ In the asymptotic limit $\epsilon \xrightarrow{R \rightarrow \infty} cte$ predicted by K41, the dissipative range extends up to $k_{dis} \rightarrow \infty$
- ✓ Consistent with this, the accumulated enstrophy becomes

$$\Omega = \int_{k_0}^{k_{dis}} k^2 E(k) dk \approx \epsilon^{2/3} k_{dis}^{1/3} \quad \Rightarrow \quad \Omega \approx \frac{\epsilon}{\nu}$$

Number of degrees of freedom

- How many degrees of freedom are required to describe a turbulent flow ?

$$N = \left(\frac{\ell_0}{\ell_{dis}}\right)^D$$
- Since $\Rightarrow R = \frac{u_0 \ell_0}{\nu}$ and $u_0 = (\varepsilon \ell_0)^{1/2}$
- We obtain $\Rightarrow N = R^{3/2}$

Numerical requirements


- The memory requirements for the simulation of turbulent flows, scale like N.
- The number of integration steps also increases with the Reynolds number. To resolve the shorter timescales

$$N_t = \frac{T}{dt} = \nu k_{dis}^2 T \approx R^{3/2}$$
- The requirement of CPU, measured as the number of floating point operations, scales like

$$N_{FP} = N \cdot N_t \approx R^{3/2} R^{3/2}$$

Our numerical simulations

- We perform 2D and 3D simulations of the incompressible Navier-Stokes eqn., assuming periodic boundary conditions.
- We use pseudo-spectral techniques to compute the spatial derivatives.
- We use a 2nd order Runge-Kutta scheme for the time integration.
- For the 3D runs we use a parallel version compiled with MPI (message passing interface)
- 3D simulations are run on **bocha**, a cluster of 40 nodes set up at the Department of Physics (<http://cesen.df.uba.ar/>).



2D flows

- In incompressible 2D flows, the velocity field can be derived from a stream function, i.e.

$$\vec{u} = \nabla \times (\hat{z} \phi)$$
- The stream function satisfies the following equation

$$\frac{\partial \omega}{\partial t} = [\phi, \omega] + \nu \nabla^2 \omega, \quad \text{where } \omega = -\nabla^2 \phi$$
- The ideal invariants for this equation, are

$$E = \int d^2x \frac{|\vec{u}|^2}{2} = \frac{1}{2} \sum_{\vec{k}} k^2 |\phi_{\vec{k}}|^2 \quad \text{energy}$$

$$\Omega = \int d^2x \frac{\omega^2}{2} = \frac{1}{2} \sum_{\vec{k}} k^4 |\phi_{\vec{k}}|^2 \quad \text{enstrophy}$$

2D flows: ideal invariants

- When viscosity is considered, the dissipation of energy and enstrophy is described by

$$\frac{dE}{dt} = -2\nu\Omega, \quad \frac{d\Omega}{dt} = -2\nu P$$
 where $P = \int d^2x |\nabla \times (\nabla \times \vec{u})|^2 = \frac{1}{2} \sum_{\vec{k}} k^4 |\phi_{\vec{k}}|^2$ *palinstrophy*
- Theorem:** An incompressible 2D flow satisfies $\left| \frac{\Omega}{E} \right| > \left| \frac{\dot{E}}{E} \right|$
- Dem.:** Let us start from $\sum_{\vec{k}} k^2 k'^2 (k^2 - k'^2)^2 |\phi_{\vec{k}}|^2 |\phi_{\vec{k}'}|^2 \geq 0$
- Using definitions of E, Ω and P $\Rightarrow P E \geq \Omega^2$
- and since $|\dot{E}| = 2\nu\Omega$, $|\dot{\Omega}| = 2\nu P \Rightarrow \left| \frac{\Omega}{E} \right| > \left| \frac{\dot{E}}{E} \right|$

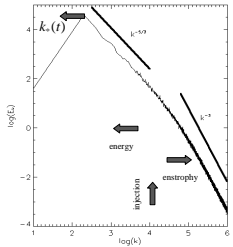
Direct and inverse cascades

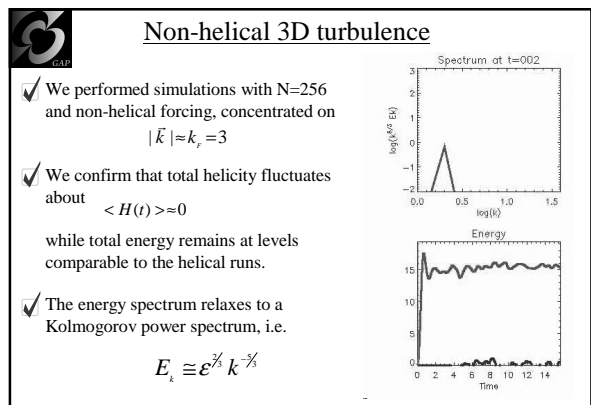
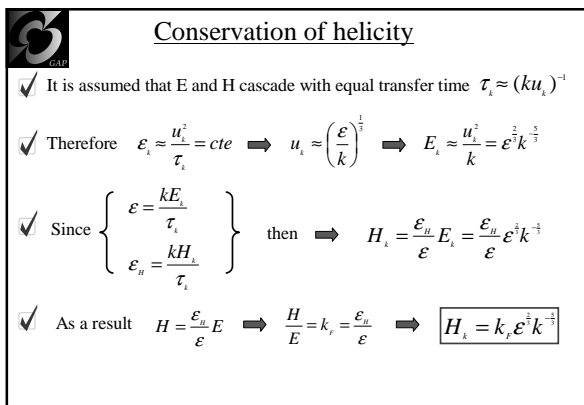
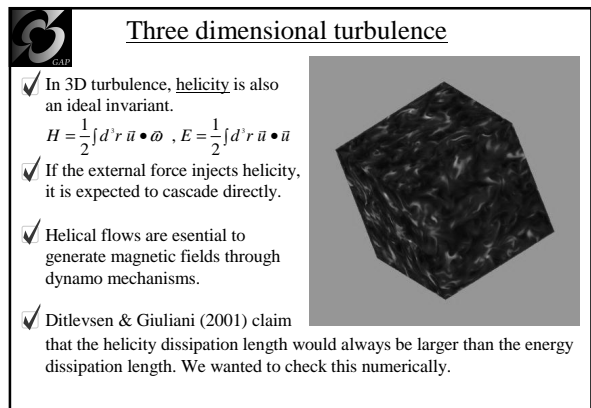
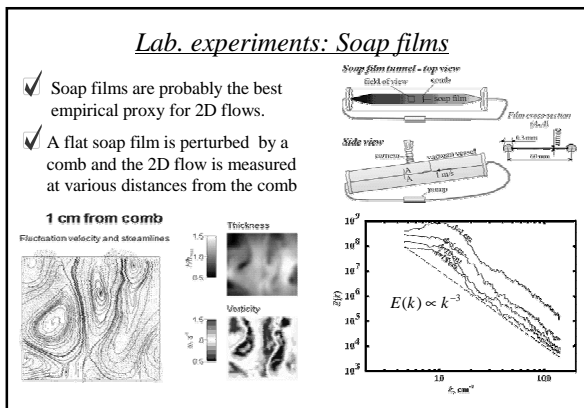
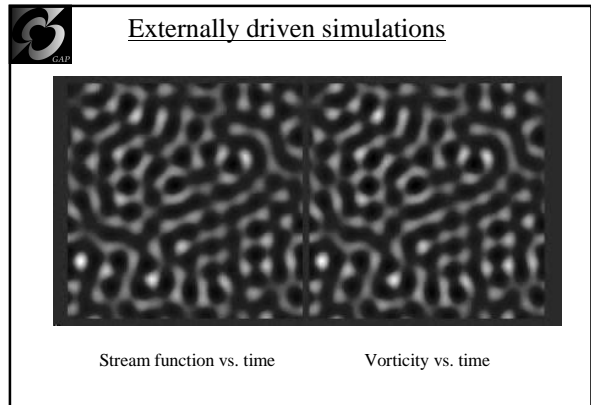
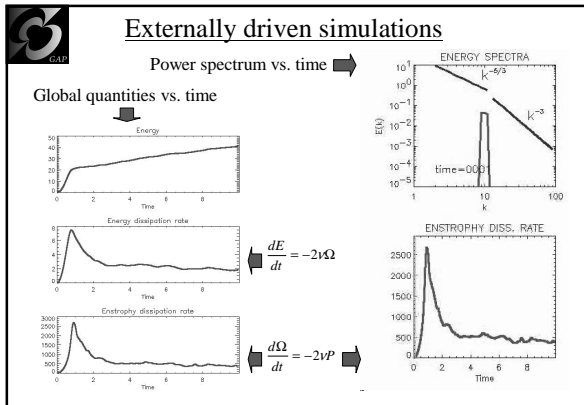
- The previous theorem shows that Ω is more fragile than E. As a result, Ω is expected to cascade directly, while E follows an inverse cascade.
- For the direct enstrophy cascade

$$\varepsilon_{\Omega} \approx \frac{\omega_k^2}{\tau_k} = const. \quad , \quad E_k \approx \frac{u_k^2}{k}$$

$$E(k) = (\varepsilon_{\Omega})^{2/3} k^{-3}$$
- Because of the inverse cascade, energy accumulates at large scales, with $k_s(t)$ progressing like

$$E(t) = \int_{k_s(t)}^{k_w} dk E(k) \approx \varepsilon t \Rightarrow k_s(t) \approx \varepsilon^{-1/2} t^{-3/2}$$

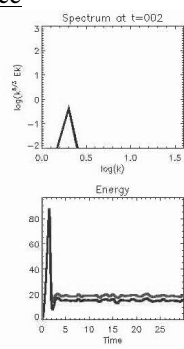




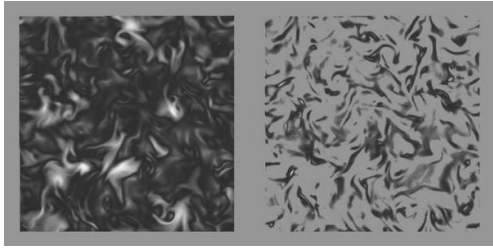
Helical 3D turbulence

- ✓ We apply helical forcing (ABC flow) to all Fourier modes with $|\vec{k}| \approx k_r = 3$
- ✓ We obtain direct energy and helicity cascades (as conjectured by Brassaud et al. 1973).
- ✓ We confirm the helicity spectrum obtained by Borue & Orszag 1997, i.e.

$$H_i \cong \frac{\epsilon_H}{\epsilon} E_i, \quad \frac{\epsilon_H}{\epsilon} \approx k_r, \quad E_i \cong \epsilon^{2/3} k^{-5/3}$$
- ✓ However, we find that the dissipation scales are equal, and therefore microscopic flows in helical turbulence, are also helical!



Helical 3D turbulence



Slice of energy Slice of helicity

Conclusions

- ✓ We presented a general overview of our current understanding of hydrodynamic turbulence.
- ✓ Several experimental results are consistent with Kolmogorov's power spectrum.
- ✓ We presented numerical simulations of 2D turbulence which confirm a direct enstrophy cascade and an inverse energy cascade.
- ✓ Our 3D simulations confirm the presence of direct cascades of both energy and helicity, with a K41 power spectrum.
- ✓ Simulations also show that helicity dissipates at the same scale as energy. This persistence of helical motions at small scales is important for dynamo mechanisms to operate.